Chemical Physics Letters 618 (2015) 57–62

Contents lists available at ScienceDirect

Chemical Physics Letters

journal homepage: www.elsevier.com/locate/cplett

Ab initio study of adsorption properties of hazardous organic molecules on graphene: Phenol, phenyl azide, and phenylnitrene

Junsu Lee, Kyung-Ah Min, Suklyun Hong, Gunn Kim*

Department of Physics and Graphene Research Institute, Sejong University, Seoul 143-747, South Korea

ARTICLE INFO

Article history:
Received 12 September 2014
In final form 28 October 2014
Available online 4 November 2014

ABSTRACT

Phenol, phenyl azide, and phenylnitrene are hazardous organic molecules; therefore, the fabrication of sensors or filters with high sorption capabilities for the chemicals is necessary. Considering van der Waals interaction, we perform first-principles density functional theory calculations to investigate the adsorption properties of the hazardous molecules on graphene. For parallel stacking configurations, AB stacking is slightly more favorable than AA stacking for all the adsorbates that we considered. We find that phenyl azide has a higher adsorption energy than phenol. Phenylnitrene forms covalent bonds with graphene in oblique stacking structures, resulting in a bandgap opening in graphene.

1. Introduction

Graphene has attracted much attention because it has unique properties [1–8]. Its very large surface area is an important property, and has enabled the development of various applications, including filters for removing toxic compounds, and chemical sensors for detecting molecules at small concentrations. The binding properties of hazardous molecules on graphene have been examined theoretically and experimentally for potential applications to filters and sensors [9,10].

Phenol has an aromatic ring structure with a hydroxyl group (—OH) [11], and forms a colorless-to-white solid when it is pure. It becomes reddish when exposed to air. Phenol is produced from coal tar or petroleum, and used as a precursor in the manufacture of plastics and numerous pharmaceutical drugs. The substance is a well-known toxic water pollutant. Prolonged contact with phenol vapor is harmful to the skin (dermatitis and skin burns), and repeated exposure to phenol may damage the heart, lung, liver, brain, and kidneys [12,13].

Phenyl azide, which is a prototypical organic azide, has an aromatic phenyl group. It consists of a linear azide group ($-N_3$) connected to a phenyl group. Phenyl azide is explosive, and therefore extra care must be taken during purification and handling. Phenylnitrene can be generated by thermolysis or photolysis of phenyl azide, with expulsion of nitrogen gas [14,15]. Nitrenes are generally reactive intermediates and are involved in many chemical reactions. Phenylnitrene has a very short lifetime: ~1 ns.

In this letter, we report the results of an *ab initio* investigation of adsorption of phenol, phenyl azide, and phenylnitrene on a graphene monolayer. For comparison with the adsorption properties of the hazardous organic molecules and radical, we also investigate the atomic and electronic structures of benzene on a graphene monolayer. For parallel stacking configurations, we focus on AA and AB stacking between the benzene derivative and the graphene hexagons, and the adsorption energies between them. In addition, we consider the oblique stacking structures of phenylnitrene, and show that it bonds covalently with graphene, because of the dangling bond of the nitrogen atom in the radical in oblique stacking. We also investigate the electronic properties of benzene, phenol, phenyl azide, and phenylnitrene on graphene.

2. Computational details

We studied the structural and electronic properties of the adsorbates on graphene using density functional theory [16]. We utilized a plane-wave basis set and the projector augmented wave [17], implemented using the Vienna ab initio simulation package (VASP) [18]. The cutoff energy for the kinetic energy was 500 eV, and the generalized gradient approximation (GGA) was used to describe the exchange-correlation energy functional of the Perdew–Burke–Ernzerhof (PBE) form [19]. In general, chemical bonding and electron transfer can be described well within the GGA. However, dispersion and van der Waals (vdW) forces are not represented well by the GGA functional, because quantum electronic interactions in the regions of low electron densities

* Corresponding author.
E-mail address: gunnkim@sejong.ac.kr (G. Kim).

http://dx.doi.org/10.1016/j.cplett.2014.10.064
0009-2614/

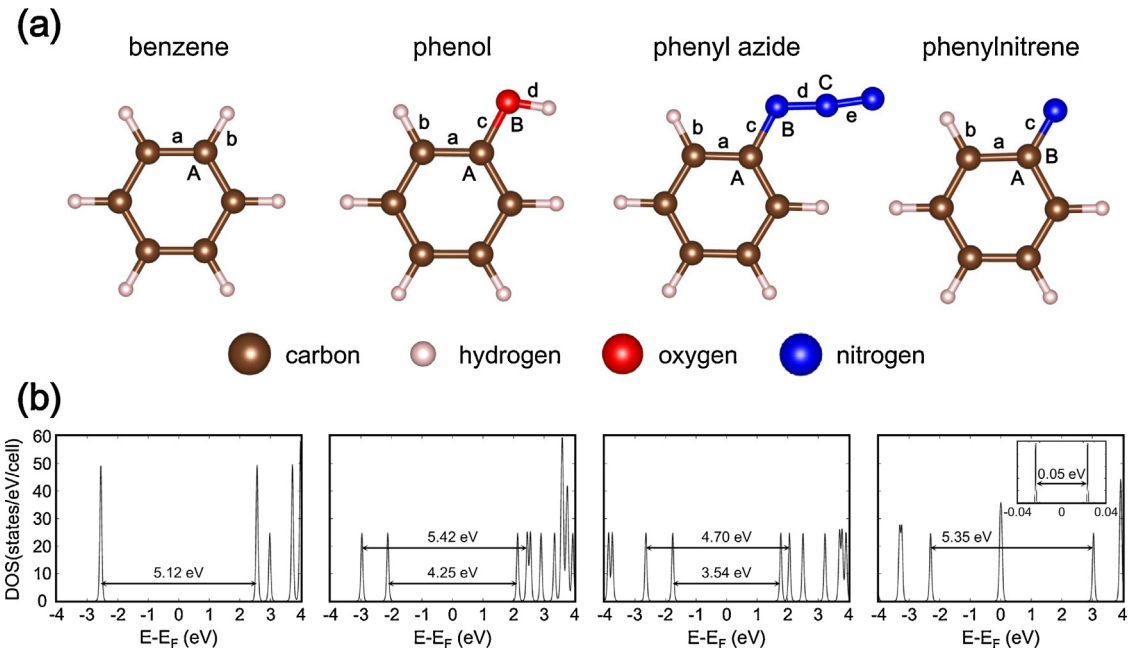

Figure 1. (a) Model structures and (b) DOSs of benzene, phenol, phenyl azide, and phenylnitrene from left to right, respectively.

are not correctly expressed. In the calculations, we considered vdW interaction between the adsorbates and graphene, using Grimme's DFT-D2 [30], Tkatchenko–Scheffler (TS) [20] and optB86b [21,22] methods within the PBE-type functional. Adsorption of organic molecules on graphene has been widely studied using the dispersion-corrected DFT calculations with various vdW functionals [23–27]. It is also very important to consider the vdW correction in layered structure such as graphite and black phosphorus [28,29]. We used the Quantum ESPRESSO package to plot the wavefunctions for phase information. The cutoff energy for the kinetic energy was 408 eV (30 Ry). As in the calculations using the VASP code, we adopted a PBE-type exchange-correlation energy functional.

A 6×6 unit cell was chosen for graphene, and the C—C bond length was 1.42 Å. In the relaxation of all model systems, $4 \times 4 \times 1$ Monkhorst–Pack sampling [31] was used for the Brillouin-zone integrations. We used $25 \times 25 \times 1$ k points to compute the densities of states (DOSs) of the model systems. For the isolated molecules (phenol, phenyl azide, and phenylnitrene), shown in Figure 1, only one k point at the Γ point was used for the unit cell calculation. The DOS of each molecule was plotted for comparison (Figure 1). We obtained the adsorption energy for each configuration, (E_{ad}), defined by

$$E_{ad} = E[\text{graphene}] + E[\text{molecule}] - E[\text{graphene} + \text{molecule}],$$

where E[graphene + molecule] and E[graphene] are the total energies of the graphene sheet with and without an adsorbate molecule, respectively, and E[molecule] represents the energy of an isolated molecule.

Among many parallel stacking configurations, we concentrated on AA and AB stacking types, as shown in Figure 2. In AA stacking, the aromatic ring of the adsorbate faces the graphene hexagons, and the oxygen (or nitrogen) atom binding to the phenyl group is on top of a graphene carbon atom. In AB stacking, in contrast, the center of the aromatic ring of the molecule is on top of a graphene carbon atom; this is similar to the Bernal stacking of graphite. We consider two different configurations (AB1 and AB2) for the AB stacking, according to the relative position of the side group bound to the phenyl group. The difference between AB1 and AB2

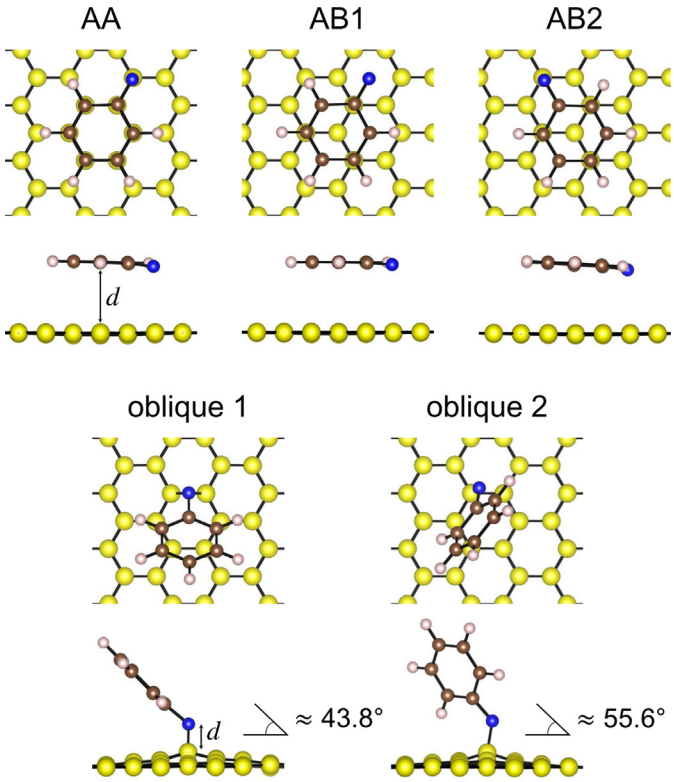

Figure 2. Model structures for adsorption of phenylnitrene on graphene monolayer. In AA stacking, the aromatic ring of the adsorbate faces the graphene hexagons directly. In AB stacking, similar to Bernal stacking of graphite, the center of the aromatic ring of the molecule is on top of a graphene carbon atom. Here, d represents the distance between the adsorbate and the graphene layer. AB1 and AB2 are distinguished by the relative positions of the side groups bound to the phenyl groups. Phenylnitrene has other configurations (oblique 1 and 2 stacking), arising from the dangling bond in the radical. After geometry optimization using the DFT-D2 method, the tilting angles are 43.8° and 55.6° for the oblique stacking structures.

Table 1
Bond lengths (Å) and angles (°) in benzene, phenol, phenyl azide, and phenylnitrene in the gas phase. The labels for bonds (a, b, c, d, and e) and angles (A, B, and C) are explained in Figure 1.

	Benzene	Phenol	Phenyl azide	Phenylnitrene
a	1.40	1.40	1.40	1.46
b	1.09	1.09	1.09	1.09
c	–	1.38	1.42	1.29
d	–	0.97	1.23	–
e	–	–	1.15	–
A	120.0	120.2	120.3	116.8
B	–	108.9	119.2	121.6
C	–	–	173.0	–

is whether the oxygen (or nitrogen) atom binding to the phenyl group is on top of a graphene carbon atom or on top of the center of a graphene hexagon. The oblique stacking configurations of phenylnitrene were also taken into account, because the nitrogen atom connected to the phenyl group has broken bonds. For oblique 1 stacking of phenylnitrene, the broken bond disappears and the nitrogen atom of phenylnitrene is bonded to two carbon atoms in graphene, i.e., it has a bridge-site configuration. In the case of oblique 2 stacking of phenylnitrene, the nitrogen atom is bonded to one carbon atom at the top of graphene.

3. Results and discussion

First, we examine the structural and electronic properties of the individual molecules in the gas phase. Figure 1(a) shows the optimized geometries of benzene, phenol, phenyl azide, and phenylnitrene. Table 1 summarizes the bond lengths and bond angles of the molecules. In phenyl azide and phenylnitrene, the C—N bond becomes stronger when a N_2 molecule is removed by photolysis. The data in Table 1 show that the bond angles in phenylnitrene evidently differ from those in the other molecules.

Figure 1 shows the DOSs of all the molecules and radical that we considered. The highest occupied molecular orbital–lowest unoccupied molecular orbital (HOMO–LUMO) gaps are 5.12, 4.25, and 3.54 eV for benzene, phenol, and phenyl azide, respectively. This is because the HOMOs and LUMOs for benzene and phenol are mainly in the aromatic ring (phenyl group), and have almost the same wavefunctions. For benzene, the HOMO and LUMO are both doubly degenerate. In contrast, for phenyl azide, the electron density of the LUMO is distributed on the N_3 side group, and the LUMO+1 of phenyl azide is very similar to that of the LUMO of benzene. The energy spacing between LUMO and LUMO+1 is small (~0.3 eV) in this case. The wavefunctions are presented in Figure 3. The HOMO–LUMO gap of phenylnitrene is only 0.05 eV, because its HOMO and LUMO originate mainly from a nitrogen atom with a dangling bond. The HOMO-2 and LUMO+1 of phenylnitrene have similar wavefunctions to the HOMO and LUMO of benzene, respectively, and the energy spacing between the two levels is 5.35 eV, as shown in Figure 1. The partial charge densities (the absolute square of the wavefunctions) of phenylnitrene are shown in Figure 4.

Table 2 summarizes the adsorption energies (E_{ad}) and separation (d) for all the adsorption configurations. In this calculation, we considered three vdW functionals (i.e., DFT-D2, TS, and optB86b-vdW). Among the three method for the vdW scheme, optB86b-vdW produces highest adsorption energy (E_{ad}), whereas DFT+D2 has the lowest adsorption energy for the same stacking configuration. For all molecules, AB stacking is slightly more stable than AA stacking, regardless of vdW functionals. The adsorption energies of the AA and AB configurations of benzene are higher than the results (~0.3 eV) obtained using the local density approximation [32,33]. An experimental study using thermal desorption spectroscopy demonstrated that the desorption kinetics of benzene at submonolayer coverage yields an activation energy of 0.5 ± 0.08 eV [34]. In a previous dispersion-corrected DFT study with the DFT-D method, they obtained an adsorption energy of ~0.49 eV, which agrees with the experimental value in the case of benzene AB [35]. According to Berland and Hyldgaard, the adsorption separation and energy are sensitive to the exchange variant used in vdW correction [36]. Earlier theoretical studies also showed that the AB (hollow site) configuration is more stable. The atom-resolved projected density of states (PDOS) can account for the stacking-dependent adsorption properties of the organic molecules on graphene. As shown in Supplementary data, the adsorption energy increases as p_z orbital hybridization between the molecule and graphene becomes stronger, which can explain the fact that AB1 has the larger binding energy than that of AB2 for benzene, phenol, and phenyl azide. In contrast, AB2 is more stable than AB1 in phenylnitrene because of the dangling bond of the N atom.

In vdW-DF calculations for phenol-adsorbed graphite, Chakarova-Käck et al. showed that the adsorption energies are 0.56 and 0.55 eV for the AB1 and AB2 configurations, respectively [37]. Similar to the phenol case, the AB1 configuration is slightly more favorable than AB2 for the considered vdW schemes. Interestingly, phenyl azide has a higher adsorption energy than phenol. In contrast, for phenylnitrene, the AB2 configuration is slightly more favorable than AB1 for π stacking. This can be ascribed to the dangling bond of the nitrogen atom in phenylnitrene (Figure 2).

We also consider two types of oblique stacking structures, as shown in Figure 2. In oblique 1 stacking, with a tilting angle of 43.8° obtained by the DFT-D2 method, the C—N bond length between the carbon atom in graphene and the nitrogen atom in phenylnitrene is 1.49 Å, and the C—C bond lengths for the two carbon atoms bonded to the nitrogen atom in phenylnitrene are 1.55 Å (a single bond). In this case, covalent functionalization occurs, resulting in a much higher adsorption energy of 1.48 eV than π stacking. K. Suggs et al. considered only oblique 1 stacking of perfluorophenylazide (PFPA) [38]. In their model, PFPA forms an aziridine adduct [39] by cycloaddition with carbon-carbon bonds in graphene. However, they did not give careful consideration to an atop-site oblique stacking like our oblique 2 stacking. In our study, oblique 2 stacking, with a tilting angle of 55.6° obtained by the DFT-D2 method, has an adsorption energy of 1.71 eV, as shown in Table 2. It means that oblique 2 stacking has the lower total energy than oblique 1 stacking by 0.23 eV, although a broken bond is present. For oblique 1 stacking, the N atom is bonded to two C atoms in graphene, and the ∠CNC bond angle is ~60°, which is much smaller than the ∠HNH angle (~120°) in the gas-phase aniline ($C_6H_5NH_2$) molecule. In oblique 2 stacking, the C—N bond length between the carbon atom in graphene and the nitrogen atom in phenylnitrene is 1.49 Å, which is the same as in oblique 1 stacking, as shown by the data in Table 2. In Table 2, we also obtain the adsorption energies and separation for phenylnitrene with the TS, optB86b method and without vdW (w/o vdW) corrections. The general trend is practically the same, regardless of the vdW scheme, as shown in Table 2.

In a benzene-adsorbed graphene layer, the AA and AB stacking configurations have very similar electronic structures, because both are weak π stacking. The DOS of the AB-type case is shown in Figure 3(a). The Dirac point coincides with the Fermi level, which means that no significant charge donation takes place between benzene and graphene. Furthermore, we find no bandgap opening as a result of adsorption of benzene on graphene. These observations are in good agreement with previous reports [32,33]. States A and B (C and D) are nearly degenerate at around −2 eV (+3 eV), and they originate from the doubly degenerate HOMO (LUMO) of the benzene molecule. We can determine the mirror (reflection) symmetry of benzene from its energy eigenfunctions. States A and B have a nodal plane, parallel to the yz and zx planes, respectively, as shown in Figure 3. In the cases of states C and D, two nodal

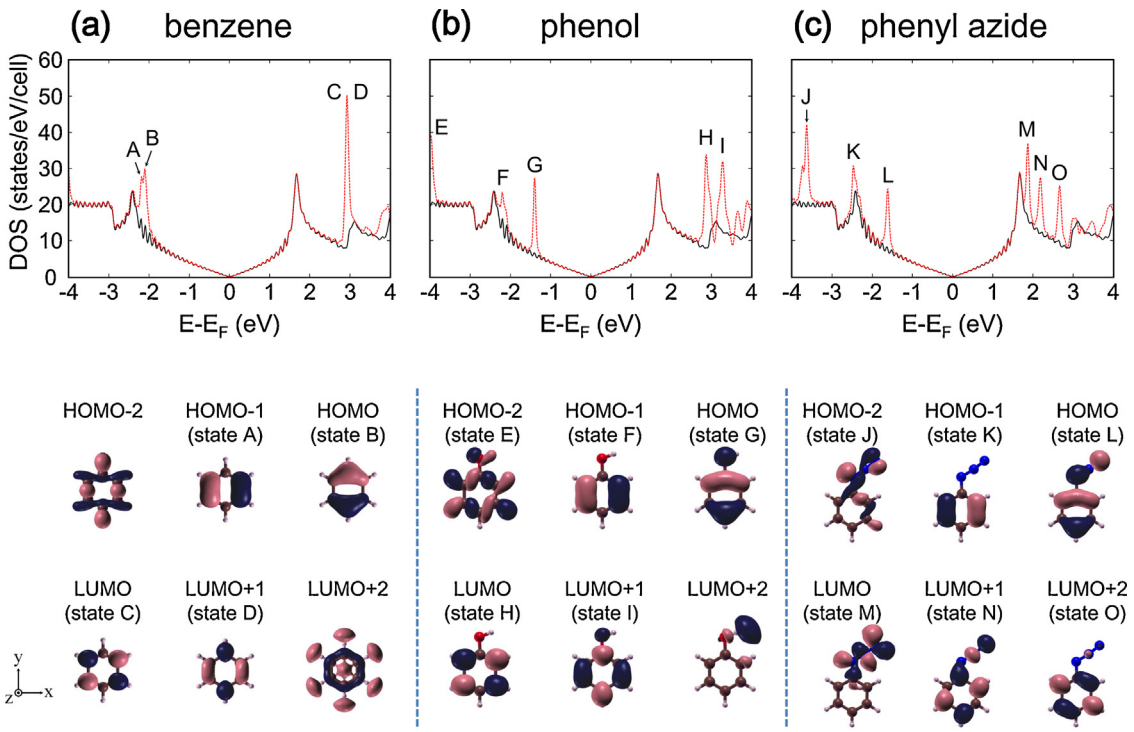

Figure 3. DOS plots and molecular orbitals (from HOMO-2 to LUMO+2) of (a) benzene-adsorbed graphene, (b) phenol-adsorbed graphene, and (c) phenyl azide-adsorbed graphene. Black and red curves denote the DOSs of bare graphene and graphene with adsorbate molecules, respectively. (For interpretation of the references to color in this figure legend, the reader is referred to the web version of this article.)

planes are present. For the LUMO+2 of the benzene molecule on graphene, shown in Figure 3(a), there are nodes between the carbon and hydrogen atoms, and this means that the C—H bond exhibits antibonding characteristics.

In a phenol-adsorbed graphene layer, states E, F, G, H, and I are delocalized states on the phenyl group, and they are almost the same as the states in benzene. In contrast, the LUMO+2 for phenol is a localized state on the hydroxyl (—OH) group, which is out of the range in Figure 3. The phenyl azide-adsorbed graphene layer has six localized states, in the energy range −4 eV to +4 eV. The electron densities of states J and M are mainly localized on the azide ($—N_3$) group. State L is the HOMO of phenyl azide and is similar

Table 2
Adsorption energies (E_{ad}) and separations (d) of benzene, phenol, phenyl azide, and phenylnitrene on a graphene monolayer with three vdW schemes: DFT-D2, TS and optB86b. For oblique stacking of phenylnitrene, we also obtained E_{ad} and d without vdW (w/o vdW). For parallel stacking, the adsorption separation is the average distance between the aromatic molecule and graphene in the z direction. For oblique stacking of phenylnitrene, the adsorption separation represents the C—N bond length.

	DFT-D2	TS	optB86b	DFT-D2	TS	optB86b
	Benzene AA			Benzene AB		
E_{ad} (eV)	0.38	0.55	0.56	0.42	0.59	0.60
d (Å)	3.35	3.37	3.35	3.22	3.31	3.30
	Phenol AA			Phenol AB1		
E_{ad} (eV)	0.42	0.61	0.63	0.49	0.68	0.69
d (Å)	3.35	3.39	3.40	3.23	3.32	3.29
	Phenol AB2			Phenyl azide AA		
E_{ad} (eV)	0.46	0.66	0.67	0.50	0.71	0.75
d (Å)	3.25	3.33	3.31	3.36	3.41	3.36
	Phenyl azide AB1			Phenyl azide AB2		
E_{ad} (eV)	0.56	0.77	0.80	0.54	0.75	0.78
d (Å)	3.23	3.33	3.30	3.26	3.33	3.32
	Phenylnitrene AA			Phenylnitrene AB1		
E_{ad} (eV)	0.53	0.70	0.75	0.55	0.73	0.76
d (Å)	3.29	3.35	3.33	3.23	3.30	3.28
	Phenylnitrene AB2					
E_{ad} (eV)	0.59	0.75	0.80	–	–	–
d (Å)	3.19	3.29	3.22	–	–	–

	DFT-D2	TS	optB86b	w/o vdW	DFT-D2	TS	optB86b	w/o vdW
	Phenylnitrene oblique 1				Phenylnitrene oblique 2			
E_{ad} (eV)	1.48	1.45	1.58	0.94	1.71	1.70	1.82	1.26
d (Å)	1.49	1.49	1.49	1.48	1.49	1.49	1.49	1.49
tilting angle (°)	43.8	43.7	43.3	46.2	55.6	55.5	55.5	55.5
∠ CNC angle (°)	62.8	62.5	62.4	63.3	–	–	–	–

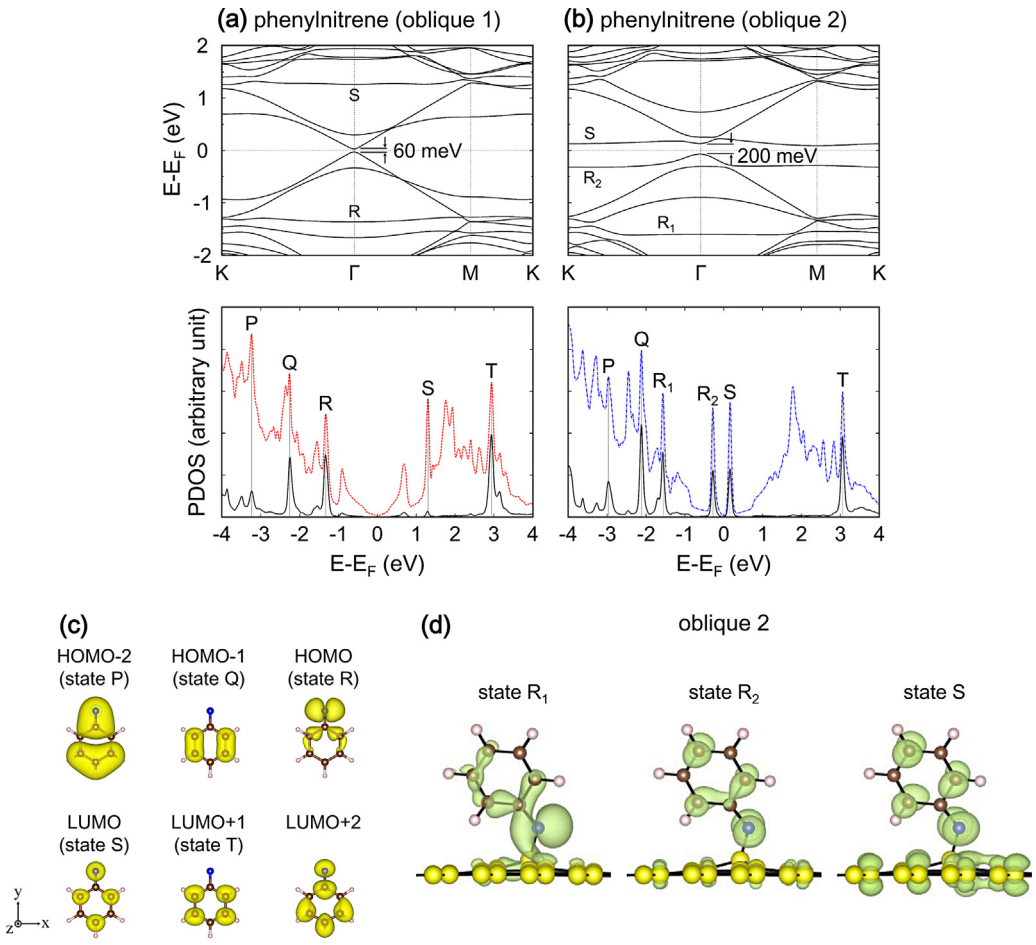

Figure 4. Band structures and PDOSs of phenylnitrene-adsorbed graphene with (a) oblique 1 stacking and (b) oblique 2 stacking. (c) Partial charge densities of molecular orbitals of phenylnitrene (from HOMO-2 to LUMO+2). Partial charge densities of states R and S for oblique 1 stacking are shown in (d) and (e), respectively. Black, red, and blue curves denote the PDOSs of the phenylnitrene radical, phenylnitrene-adsorbed graphene with oblique 1 and oblique 2 stackings, respectively. (For interpretation of the references to color in this figure legend, the reader is referred to the web version of this article.)

to the HOMO of benzene. In this case, the nitrogen atom at the center of the azide group has no electron density. State M is the LUMO of phenyl azide, and exhibits antibonding characteristics for the nitrogen atoms, which have alternating signs in the molecular orbitals. State N is similar to the LUMO of benzene. The nitrogen atom bonded to the aromatic ring has no electron density for state N.

Finally, we study a graphene monolayer with phenylnitrene. Nitrenes can functionalize graphene [39,40], because they are highly reactive intermediates, by thermal or photochemical activation of organic azides. Many researchers have already used nitrene chemistry for the chemical modification of carbon nanotubes and fullerenes [41,42]. As phenylnitrene has a broken bond, vertical stacking as well as parallel stacking is considered. Our results show that such chemical functionalization of phenylnitrene gives rise to a bandgap opening in graphene, and the graphene monolayer is weakly p-doped for oblique 2 stacking. A bandgap of $\approx$ 60 meV ($\approx$ 200 meV) occurs in graphene with oblique 1 (oblique 2) stacking with phenylnitrene, as shown by the band structures (Figure 4(a) and (b)). In a higher coverage, the highly p-doped graphene sheet would be produced with a larger bandgap. Figure 4(a) and (b) also shows the PDOSs of the phenylnitrene-adsorbed graphene monolayers with oblique 1 and oblique 2 stackings, respectively. The peaks in the DOS correspond to the molecular orbitals in Figure 4(c). We failed to obtain the wavefunctions with phase information for the molecular orbitals of phenylnitrene using the Quantum Espresso code. This may be because the two states, HOMO and LUMO, are very close. However, we obtained partial charge density without phase information using the VASP code. The HOMO and LUMO are strongly localized states, and they correspond to states R and S in the DOS. The HOMO is around −1.3 eV for state R (−1.3 eV for state R_1 and −0.3 eV for state R_2), and the LUMO is around +1.3 eV (+0.2 eV) for oblique 1 (oblique 2) stacking. In oblique 2 stacking, one dangling bond remains, and hence the energy levels of the HOMO and LUMO are near the Fermi level. In the case of parallel stacking (π stacking) of phenylnitrene, the broken bond survives and the localized states (R and S) originating from phenylnitrene are at the Fermi level (not shown in the DOSs).

4. Conclusion

Considering vdW interaction, we have investigated the adsorption of benzene, phenol, phenyl azide, and phenylnitrene on graphene using the DFT method. In parallel (π) stacking, all the molecules adsorbed on graphene have weak vdW interactions with graphene for both AA and AB stacking structures. Phenyl azide binds to graphene more strongly than phenol. In particular, phenylnitrene, which has an oblique stacking structure, has stronger interactions with graphene, representing covalent bonding with a bandgap opening in graphene. Consequently, our theoretical study demonstrates that the chemical doping of phenylnitrene can tailor the band structure of graphene. Besides, an oblique stacking structure where the N atom in phenylnitrene is bonded to one C atom in the graphene (an atop site) is energetically more

stable than another oblique stacking structure where the N atom is bonded to two C atoms in graphene (a bridge site). In the application of graphene-based sensors to detect the hazardous organic molecules, significant charge transfer or chemical doping should occur between graphene and adsorbates. Since no remarkable charge donation and band structure change are shown in our calculation, it is difficult to use graphene for sensing benzene, phenol, and phenyl azide. However, graphene can still be used for filtering the compounds. In contrast, phenylnitrene can give rise to the bandgap opening of graphene, and therefore graphene can act as a sensor for the phenylnitrene radical.

Acknowledgments

The authors acknowledge the support of the Basic Science Research Program through the National Research Foundation of Korea (NRF) (Grant No. 2013R1A1A2009131) and the Priority Research Center Program (Grant No. 2010-0020207) funded by the Ministry of Education, and Nano Material Technology Development Program (2012M3A7B4049888) through the NRF funded by the Ministry of Science, ICT and Future Planning.

Appendix A. Supplementary data

Supplementary data associated with this article can be found, in the online version, at http://dx.doi.org/10.1016/j.cplett.2014.10.064.

References

[1] K.S. Novoselov, et al., Science 306 (2004) 666.
[2] K.S. Novoselov, et al., Nature (London) 438 (2005) 197.
[3] Y. Zhang, Y.-W. Tan, H.L. Stormer, P. Kim, Nature (London) 438 (2005) 201.
[4] M.I. Katsnelson, K.S. Novoselov, A.K. Geim, Nat. Phys. 2 (2006) 620.
[5] A.F. Young, P. Kim, Nat. Phys. 5 (2009) 222.
[6] V.V. Cheianov, V. Fal'ko, B.L. Altshuler, Science 315 (2007) 1252.
[7] A. Rycerz, J. Tworzydło, C.W.J. Beenakker, Nat. Phys. 3 (2007) 172.
[8] C. Park, et al., Proc. Natl. Acad. Sci. U.S.A. 108 (2011) 18622.
[9] F. Schedin, A.K. Geim, S.V. Morozov, E.W. Hill, P. Blake, M.I. Katsnelson, K.S. Novoselov, Nat. Mater. 6 (2007) 652.
[10] O. Leenaerts, B. Partoens, F.M. Peeters, Phys. Rev. B 77 (2008) 125416.
[11] J. McMurry, Organic Chemistry, 6th edn., Brooks Cole, 2003.
[12] M.A. Warner, J.V. Harper, Anesthesiology 62 (1985) 366.
[13] World Health Organization/International Labour Organization: International Chemical Safety Cards, http://www.inchem.org/documents/icsc/icsc/eics0070.htm
[14] G.B. Schuster, M.S. Platz, Adv. Photochem. 17 (1992) 69.
[15] A.K. Schrock, G.B. Schuster, J. Am. Chem. Soc. 106 (1984) 5228.
[16] P. Hohenberg, W. Kohn, Phys. Rev. 136 (1964) B864.
[17] G. Kresse, D. Joubert, Phys. Rev. B 59 (1999) 1758.
[18] G. Kresse, J. Furthmüller, Phys. Rev. B 54 (1996) 11169.
[19] J.P. Perdew, K. Burke, M. Ernzerhof, Phys. Rev. Lett. 77 (1996) 3865.
[20] A. Tkatchenko, M. Scheffler, Phys. Rev. Lett. 102 (2009) 073005.
[21] J. Klimes, D.R. Bowler, A. Michaelides, J. Phys.: Condens. Matt. 22 (2010) 022201.
[22] J. Klimes, D.R. Bowler, A. Michaelides, Phys. Rev. B 83 (2011) 195131.
[23] D. Le, A. Kara, E. Schröder, P. Hyldgaard, T.S. Rahman, J. Phys.: Condens. Matter 24 (2012) 424210.
[24] J.-H. Lee, Y.-K. Choi, H.-J. Kim, R.H. Scheicher, J.-H. Cho, J. Phys. Chem. C 117 (2013) 13435.
[25] K. Berland, S.D.C. Käck, V.R. Cooper, D.C. Langreth, E. Schröder, J. Phys.: Condens. Matter 23 (2011) 135001.
[26] J. Åkesson, O. Sundborg, O. Wahlström, E. Schröder, J. Chem. Phys. 137 (2012) 174702.
[27] P.A. Denis, Chem. Eur. J. 19 (2013) 15719.
[28] J. Park, B.D. Yu, S. Hong, J. Korean Phys. Soc. 59 (2011) 196.
[29] H. Kim, J. Korean Phys. Soc. 64 (2014) 547.
[30] S. Grimme, J. Comp. Chem. 27 (2006) 1787.
[31] H.J. Monkhorst, J.D. Pack, Phys. Rev. B 13 (1976) 5188.
[32] Y.-H. Zhang, K.-G. Zhou, K.-F. Xie, J. Zeng, H.-L. Zhang, Y. Peng, Nanotechnology 21 (2010) 065201.
[33] A.Z. AlZahrani, Appl. Surf. Sci. 257 (2010) 807.
[34] R. Zacharia, H. Ulbricht, T. Hertel, Phys. Rev. B 69 (2004) 155406.
[35] E.G. Gordeev, M.V. Polynski, V.P. Ananikov, Phys. Chem. Chem. Phys. 15 (2013) 18815.
[36] K. Berland, P. Hyldgaard, Phys. Rev. B 87 (2013) 205421.
[37] S.D. Chakarova-Käck, Ø. Borck, E. Schröder, B.I. Lundqvist, Phys. Rev. B 74 (2006) 155402.
[38] K. Suggs, D. Reuven, X.-Q. Wan, J. Phys. Chem. C 115 (2011) 3313.
[39] L.-H. Liu, M.M. Lerner, M. Yan, Nano Lett. 10 (2010) 3754.
[40] J. Park, M. Yan, Acc. Chem. Res. 46 (2013) 181.
[41] M. Holzinger, et al., J. Am. Chem. Soc. 125 (2003) 8566.
[42] A. Yashiro, Y. Nishida, M. Ohno, S. Eguchi, K. Kobayashi, Tetrahedron Lett. 39 (1998) 9031.